Active Control of the Dynamics of a Dual-Spin Spacecraft

Loren Slafer* and Herbert Marbach†
Hughes Aircraft Company, El Segundo, Calif.

Active damping of both vehicle nutation and payload flexibility for a dual-spin spacecraft is achieved using the interaction of the vehicle dynamics with the on-board despun payload control system. A closed-form solution to the interaction problem is presented, deriving an analytical expression which is used to establish both the fundamental stability and the strength of the coupling. Analysis of the characteristics of the interaction leads to mass property and control system design criteria which can be used to effectively optimize the interaction and provide substantial active control. Design examples are presented which illustrate the design techniques involved in the optimization. Simulation results are presented which verify the analytical conclusions.

Nomenclature

I_{xx}, I_{yy} = total vehicle moments of inertia about transverse axes (normal to the spin axis)
I_T = effective transverse inertia $= (I_{xx} I_{yy})^{1/2}$ (for a symmetric rotor)
I^P_{zz} = payload moment of inertia about the spin axis
I^R_{zz} = rotor moment of inertia about the spin axis
I^P_{xz} = payload product of inertia between spin axis and transverse plane
r = vehicle mass properties coupling parameter $(I^P_{xz})^2/(I^P_{zz} I_{xx})$
$\omega_x, \omega_y, \omega_z$ = inertial angular rates of despun payload (rad/sec)
ω_{so} = nominal rotor spin rate (rad/sec) with payload despun ($\omega_z = 0$)
ω_n = vehicle nutation frequency (with payload despun) $= I^R_{zz}\omega_{so}/I_T$
θ_z = despun payload angle with respect to an inertial reference $\int_o^t \omega_z(s)\, ds$ (small angle approximation)
T_z = torques about the bearing axis resulting from despin control system action
$G_p(s)$ = payload control system transfer function relating sensed θ to control torque T_z
$D_R(s)$ = rigid body dynamics transfer function θ_z/T_z
$D_f(s)$ = rigid and flexible body dynamics transfer function θ_z/T_z
$H(s)$ = composite control loop transfer function excluding nutation dipole and elastic modes
ω_f = flexible mode frequency (rad/sec)
A = magnitude of system gain function $[H(j\omega)]$ evaluated at nutation frequency
Φ = phase of system gain function $[H(j\omega)]$ evaluated at nutation frequency
K = magnitude of system gain function at flexible mode frequency
α = phase of system gain function at flexible mode frequency
δ^2_f = "effective inertia" of flexible mode
ρ = flexible mode mass properties coupling parameter $= \delta^2_f/I^P_{zz}$
ζ_f = damping ratio of flexible mode
τ_{dcs} = payload control system nutation damping time constant
$\tau_{passive}$ = passive nutation damper time constant
τ_f = payload control system flexible mode damping time constant

Received April 23, 1974; revision received December 10, 1974.
Index category: Spacecraft Attitude Dynamics and Control.

*Group Head, Guidance and Control Systems Laboratory, Space and Communications Group. Member AIAA.
†Senior Scientist, Guidance and Control Systems Laboratory, Space and Communications Group. Associate Fellow AIAA.

I. Introduction

FOR a dual-spin satellite, attitude stabilization is defined as maintaining the alignment of the vehicle spin axis with the system angular momentum vector. Undesirable transient nutation motion (coning of the spin axis about the angular momentum vector) will develop from disturbances such as spacecraft attitude correction maneuvers, or from the motion of articulated payload elements. The spacecraft design constraints and criteria which establish the fundamental stability characteristics of the system (i.e., the capability of the system to asymptotically reduce spacecraft nutation rates) are well known.[1-3] For a dual-spin satellite in its nominal condition (with payload inertially despun), stability can be established from energy dissipation considerations. For a spacecraft configuration in which the rotor spin inertia exceeds the total vehicle transverse inertia, the rotor spins about the vehicle axis of maximum moment of inertia (the system minimum energy state and hence an inherently stable configuration), asymptotic stability is achieved with the inclusion of an energy dissipating passive damping mechanism located on either the spinning or despun elements. Here the nutation damping (such as is provided by a mercury filled tube mounted to the spinning rotor) will augment natural stabilizing dissipation from such elements as fuel slosh or structural flexing to improve the nutation transient settling time. For a vehicle configuration in which the rotor spins about the spacecraft axis of minimum moment of inertia (the system highest energy state), the Hughes' Gyrostat system,[1] asymptotic stability is achieved only if energy dissipation on the despun element dominates energy dissipation on the spinning rotor (which acts as a destabilizing influence, attempting to force the system to its minimum energy state). An eddy-current pendulum-type damper, mounted to the despun payload, performs the necessary nutation damping function. The Intelsat IV synchronous orbit communication satellite is an example of such a system.[4] Thus, in a Gyrostat, energy dissipation on the despun payload must both establish the fundamental system stability and also provide the desired nutation transient settling time.

This paper describes a technique which can provide substantial active nutation control through the use of control torques developed by the payload despin control system, which maintains the inertial orientation of the despun payload about the vehicle spin axis. The transverse product of inertia of the despun payload provides the control coupling path between the pitch and roll axes. Other works,[5-7] have discussed this interaction and applied techniques to measure the strength of the coupling. This paper presents a closed form, analytical solution to the control system/vehicle dynamics interaction problem, and develops a general technique to predict the basic stability of the interaction and establish design criteria to obtain the maximum damping effect. It is shown

that the stability of the interaction is determined by the control system alone, and that the strength of the coupling (defined by a closed-loop nutation damping time constant) is strongly dependent on both mass properties and control-system dynamics. In addition, the technique is extended to include evaluation of interactions between payload mounted flexible elements and the control system. Again, design criteria to ensure maximum stability margins are presented.

Section II of the paper is a review of the rotation equations of motion of a dual-spin spacecraft and develops dynamics transfer functions which characterize the interaction between the roll, pitch, and yaw motion of the vehicle. In Section III, an analytical expression is derived for the closed-loop nutation damping time constant resulting from control-system interaction. The nature of the coupling is evaluated and the general results are then extended to nonrigid dynamic interaction. In Sec. V, two examples which illustrate the design techniques to optimize the interaction for both nutation and flexible body interactions are presented.

II. System Description—Vehicle Equations of Motion

In the general dual-spin satellite concept (illustrated in Fig. 1), the despun payload is free to rotate in azimuth about the rotor bearing axis. Basic stability of spacecraft attitude is obtained through gyroscopic stiffness of the spinning rotor with a passive nutation damping mechanism (despun for the Gyrostat illustrated) providing the energy dissipation necessary to maintain the alignment of the rotor spin axis with the system angular momentum vector. Control of the inertial azimuth position of the despun payload is provided by a torque motor contained in the despin bearing assembly. Controller commands are derived by the despin control system (DCS) through determination of payload attitude errors using either spinning or despun sensors. OSO, TACSATCOM I, Intelsats III and IV, MARISAT, and ANIK I (Canadian Domestic Satellite) are examples of this type of spin-stabilized system.

The linearized differential equations describing the small-angle (payload despun), rigid-body motion of the system's four rotational degrees of freedom (three equations describe

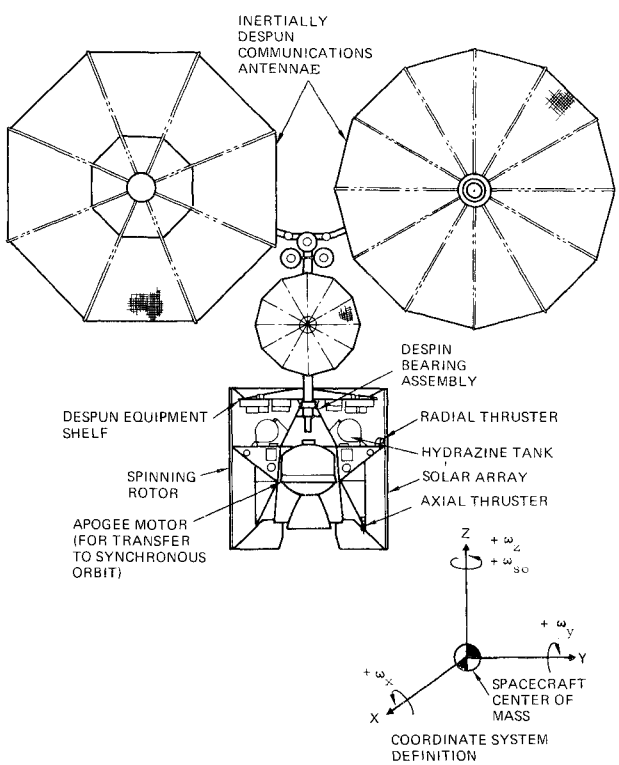

Fig. 1 Dual-spin satellite configuration.

motion of the despun payload, and a fourth describes spin motion of the rotor about the bearing axis) can be derived from Euler's equations. In the absence of external disturbance torques (and assuming a symmetric, balanced rotor), these equations become

$$\dot{\omega}_x = -[I^R_{zz}\omega_{so}/I_{xx}]\omega_y + [I^P_{xz}/I_{xx}]\dot{\omega}_z \tag{1}$$

$$\dot{\omega}_y = [I^R_{zz}\omega_{so}/I_{yy}]\omega_x \tag{2}$$

$$\dot{\omega}_z = [I^P_{xz}/I^P_{zz}]\dot{\omega}_x + [1/I^P_{zz}]T_z \tag{3}$$

$$\dot{\omega}_s = [-1/I^R_{zz}]T_z \tag{4}$$

where several simplifying assumptions have been made to clarify the present development. First, the effects of any passive nutation dampers or dedampers have been neglected for the moment, but will be included later. Secondly, only the XZ transverse product of inertia (POI) term has been included. The other transverse (YZ) POI is assumed zero through choice of axes, while the third (XY) POI is neglected for simplicity here since it is typically quite small, and in any case, does not affect the character of the results.

A brief analysis of the above equations leads to an understanding of the key role played by the POI coupling term I^P_{xz}. First note that in the absence of POI coupling, i.e., $I^P_{xz}=0$, Eqs. (1) and (2) describe the undamped oscillatory motions of the vehicle about transverse axes, with the frequency given by

$$\omega_n = I^R_{zz}\omega_{so}/I_T \tag{5}$$

This is the classical nutation mode for spin-stabilized vehicles. Also, in this case, as seen from Eq. (3), payload azimuth motions remain uncoupled from transverse nutation motions.

With a nonzero POI, on the other hand, payload azimuth and transverse motions become inertially coupled. Azimuth acceleration ($\dot{\omega}_z$) induces torque about a transverse axis, and vice versa. Thus, for the dual-spin configuration, torques (T_z) about the bearing axis developed by the payload despin control system will interact with the transverse nutation mode.

The interaction of the payload control system with the vehicle nutation mode can be evaluated by first considering the transfer function relating (for small angles) azimuth torque T_z to the payload azimuth angle θ_z

$$\int_0^t \omega_z(\tau)\mathrm{d}\tau,$$

which is the variable sensed by the control system. By taking the Laplace transform of Eq. (1) to Eq. (4), and combining terms, the following dynamics transfer functions are developed:

$$\frac{\theta_z}{T_z}(s) = \frac{1}{I^P_{zz}s^2}\left[\frac{s^2+\omega_n^2}{(1-r)s^2+\omega_n^2}\right] \tag{6}$$

$$\frac{\omega_x}{T_z}(s) = \frac{I^P_{xz}s/I_{xx}}{I^P_{zz}[(1-r)s^2+\omega_n^2]} \tag{7}$$

$$\frac{\omega_z}{\omega_x}(s) = \frac{s^2+\omega_n^2}{s^2(I^P_{xz}/I_{xx})} \tag{8}$$

where ω_n is the uncoupled nutation mode frequency defined in Eq. 5, and the inertial coupling parameter r is defined as,

$$r = (I^P_{xz})^2/I_{xx}I^P_{zz} \tag{9}$$

Note that the azimuth payload dynamics in Eq. (6) are defined by both a) the rigid body, single-axis dynamics of the controlled inertia ($1/I^P_{zz}s^2$), and b) a complex pole-zero pair

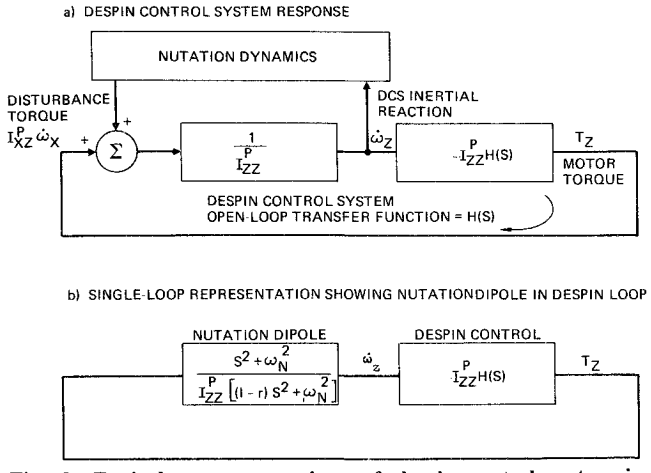

Fig. 2 Equivalent representations of despin control system interaction with nutation dynamics.

describing vehicle nutation. Note also that if there were no cross product ($I^P_{xz}=0$) the nutation pole and zero cancel, leaving only the single axis dynamics, i.e., there is no coupling path.

An additional transfer function, representing the payload despin control system dynamics, describes the derivation of control torques T_z from sensed payload angle θ_z and is defined by,

$$(T_z/\theta_z)(s)=G_P(s) \tag{10}$$

where the dynamics $G_p(s)$ are chosen to meet stability and performance requirements. The system block diagram summarizing the interaction is shown in Fig. 2.

III. Closed-Loop Interaction Analysis

The problem now becomes one of evaluating the closed-loop effect of this interaction; that is, to define the fundamental stability of the interaction and express analytically the strength of the resulting nutation damping or dedamping. The overall closed-loop system stability characteristics are determined by the system characteristic equation

$$s^2\left(1-\frac{r}{1+H(s)}\right)+\omega_n^2=0 \tag{11}$$

Note that for $H(s)=0$ (i.e., no active control) the characteristic roots are undamped and given by

$$\pm s_o=\pm j\omega_n/(1-r)^{1/2} \tag{12}$$

which becomes the classic nutation frequency with $r=0$ (or $I^P_{xz}=0$). For $H(s)\neq 0$, the roots will in general change slightly from s_o to a new value $s_o+\Delta s$. The real part of the root perturbation Δs will determine the amount of damping attributable to the DCS coupling effect.

Thus, the object now is to determine the location of the closed loop nutation roots in the s-plane; that is, the real part of the pole which defines the exponential growth or decay (stability or instability) of nutation in the coupled, closed-loop system.

Several approaches can be taken to determine Δs, and therefore the active nutation damping effect. Digital computer solution of Eq. (11) will provide an exact result, but with little or no insight as to how the character of $H(s)$ influences the interaction. Computer simulation of the vehicle equations of motion, Eqs. (1)—(4) will yield time responses of transverse rates illustrating the interaction, but again providing no insight. The approach taken here, on the other hand, makes use of the typically justifiable approximation that the perturbation of the open-loop root by closed-loop system interaction is relatively small, and yields maximum design insight with no significant loss in accuracy of the results. An illustration of the relative magnitude of the root perturbation involved in this problem is given by considering a typical application for a dual-spin satellite with a system damping time constant of 2 min (considered a 'good' design). This time constant defines the real part of the closed-loop dynamics pole as 0.0083 rad/sec. For a spacecraft with a rotor spin rate of anywhere from 20 to 120 rpm (2-12 rad/sec) the vehicle nutation frequency could be in the range of from 1-20 rad/sec (depending on configuration). Thus the shift of the open-loop nutation pole from the imaginary axis yields a closed-loop complex pole damping ratio of less than 0.008 ($\xi=1/\tau\omega n$), a very small perturbation.

Therefore, letting $s\doteq s_o+\Delta s$ in Eq. (11), solving for Δs, and neglecting second-order Δs^2 terms, we get

$$\Delta s=\frac{r\,s_o}{2[1-r+H(s_o+\Delta s)]} \tag{13}$$

By further application of the $|\Delta s|\ll|s_o|$ approximation, we make the substitution

$$H(s_o+\Delta s)\cong H\left(j\,\frac{\omega_n}{(1-r)^{1/2}}\right)\triangleq Ae^{j\emptyset} \tag{14}$$

and solve for the real part of Δs and the damping constant, with the result $(1/\tau_{dcs})=-R_e[\Delta s]$. Therefore, the nutation time constant resulting from the interaction of the control system with vehicle nutation is given by

$$\tau_{dcs}=\frac{2(1-r)^{3/2}}{r\,\omega_n}\left[\frac{1+2(A/1\text{-}r)\cos\emptyset+(A/1\text{-}r)^2}{-(A/1-r)\sin\emptyset}\right] \tag{15}$$

which can also be expressed in the form,

$$\tau_{dcs}=\frac{-2(1-r)^{3/2}}{r\,\omega_n}\,M(\bar{A},\emptyset) \tag{16}$$

(with $\bar{A}=A/(1-r)\simeq A$ for $r\ll 1$, typically the case) where $M(\bar{A},\emptyset)$ consolidates the dependence in Eq. (15) of τ_{dcs} on control-loop gain and phase shift at nutation frequency. Note the following:

1) The effects of mass properties on system damping can be isolated from the control system effects. The quantities r and $2(1-r)^{3/2}/r\,\omega_n$ are constant for a given vehicle mass properties set, while A and $\emptyset$ are variable, a result of control system design procedures.

2) For $I^P_{xz}=0$, the time constant becomes infinite; i.e., there is no effect of the control system on spacecraft nutation. This verifies the earlier observation. For $I^P_{xz}\neq 0$, the time constant varies (to first order) with $1/(I^P_{xz})^2$.

3) Since $0\leq r<1$, the sign of the time constant (implying a positive or negative nutation exponential—a stable or unstable interaction) is determined solely by the characteristics of the control system open loop transmission of nutation frequency. Selection of mass properties cannot effect the basic stability of the interaction (other than as they alter nutation frequency)—it can only modify the strength of the coupling and thus the absolute value of the resulting time constant.

By observing the sign characteristics of the function

$$M(\bar{A},\emptyset)=\frac{1+\bar{A}^2+2\bar{A}\cos\emptyset}{\bar{A}\sin\emptyset} \tag{17}$$

it can be shown that for a positive nutation time constant (hence a stable interaction resulting in active nutation damping) the transmission phase angle $\emptyset$ of nutation frequency through the system function $H(s)$ must lie in the third or fourth quadrant, i.e., $180°\leq\emptyset 360°$ for $\tau_{dcs}\leq 0$

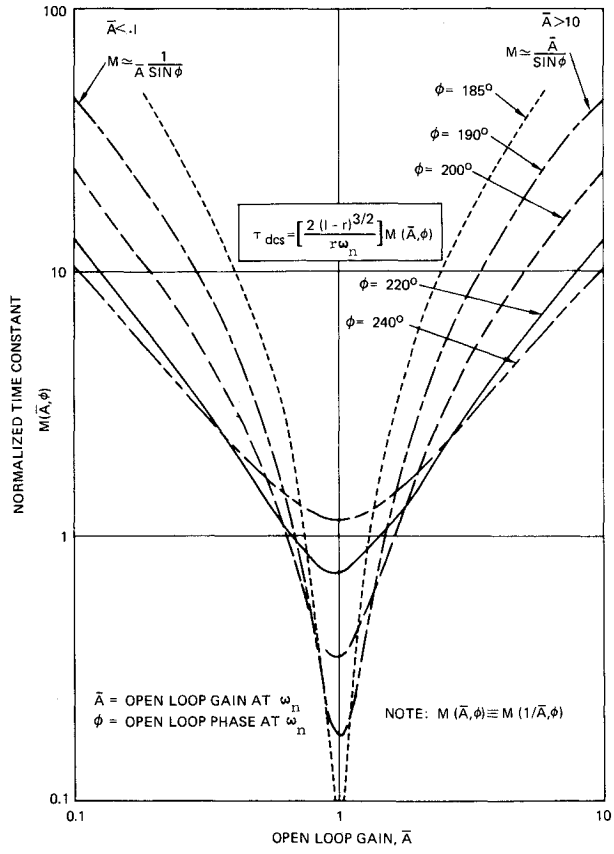

Fig. 3 Active nutation damping as a function of loop gain and phase.

In addition, it can be shown that the system coupling is weakest for both high open-loop gains ($\bar{A} \gg 1$) or low gains ($\bar{A} \ll 1$). For a gain much larger than unity, the system time constant can be approximated from Eq. (15) as

$$\tau_{dcs} \simeq \left[\frac{-2(1-r)^{3/2}}{r\,\omega_n} \right] \left[\frac{\bar{A}}{\sin \emptyset} \right] (\bar{A} \gg 1) \qquad (18)$$

i.e., τ_{dcs} increases linearly with gain (for a fixed phase angle). Similarly, for a gain much smaller than unity, the time constant can be approximated as

$$\tau_{dcs} \simeq \left[\frac{-2(1-r)^{3/2}}{r\,\omega_n} \right] \left[\frac{1}{\bar{A} \sin \emptyset} \right] (\bar{A} \ll 1) \qquad (19)$$

with τ_{dcs} increasing as A becomes smaller. In either case, the basic time constant defined by the mass properties $[2(1-r)^{3/2}/r\,\omega_n]$ is modified by the gain $\bar{A}$ (or $1/\bar{A}$) which tends to decouple the control system at the extremes of loop gain. A more detailed evaluation of the system function $M(\bar{A}, \emptyset)$ is illustrated in Fig. 3, which shows the effects on $M(\bar{A}, \emptyset)$ of changes in open-loop gain $\bar{A}$ for several values of $\emptyset$. By observing the characteristics of Eq. (15) presented in the figure, the following conclusions can be drawn. The first is that the "optimum" relationship between $\bar{A}$ and $\emptyset$ to minimize $M(\bar{A}, \emptyset)$ and hence provide maximum nutation damping, effectively tuning the control system to nutation, is to have $\bar{A} = 1$ with $\emptyset = 180.°$ This is the same condition which defines the stability constraints for the control system. Also, this condition is effectively a "saddle point" of $M(\bar{A}, \emptyset)$. For $\bar{A} \neq 1$ with $\emptyset = 180°$, τ_{dcs} becomes infinite; i.e., the system is uncoupled from nutation. The figure also shows that for a phase angle other than 180° (for "practical" designs), the optimum gain to provide the maximum possible coupling (and minimum time constant), is for the modified open loop gain $(\bar{A})$ to be as close to unity as possible.

The damping provided by a passive damping mechanism or other energy dissipation sources (such as structural flexing or fuel slosh effects) can be added directly to the active damping of the control system. The net resulting time constant can be determined from the following relationship (assuming only that τ_{dcs} and $\tau_{passive}$ are long with respect to nutation period).

$$(1/\tau_{\text{net}}) = (1/\tau_{\text{dcs}}) + (1/\tau_{\text{passive}}) \qquad (20)$$

or

$$\tau_{\text{net}} = \tau_{\text{dcs}} \tau_{\text{passive}} / \tau_{\text{dcs}} + \tau_{\text{passive}} \qquad (21)$$

This relationship is valid assuming $\omega_n \tau_{passive} \gg$, in which case the approximation

$$H\left(\frac{1}{\tau_p} + \frac{j\omega_n}{(1-r)^{1/2}} \right) \simeq H\left(\frac{j\omega_n}{(1-r)^{1/2}} \right) \qquad (22)$$

can be included in the previous analysis.

For a Gyrostat spacecraft configuration, effects such as rotor structural damping or fuel sloshing act as nutation dedampers and $\tau_{passive}$ becomes negative. This effect is analyzed in Ref. 4. To maintain attitude stability for this system (with no additional despun damping mechanism) requires

$$|1/\tau_{dcs}| > |1/\tau_{passive}| \qquad (23)$$

i.e., the net nutation time constant be positive.

IV. Application to Flexible Body Interactions

The modeling of flexible body motion using the hybrid coordinate method [8] for linear system analysis leads to a set of modal equations which can be modeled in transfer function form as shown in Fig. 4. Here the basic rigid body-dynamics block is augmented by a series of feedback loops representing the effects of the flexible body dynamics. Thus, a more complete transfer function which describes both rigid and nonrigid payload motion is given by (assuming here for simplicity a single flexible mode and with $\omega_f \gg \omega_n$)

$$\frac{\Theta_z}{T_z}(s) \equiv D_f(s) = \frac{1}{I^P_{zz} s^2} \left[\frac{s^2 + \omega_n^2}{(1-r)s^2 + \omega_n^2} \right] \left[\frac{s^2 + 2\xi_f \omega_f s + \omega_f^2}{s^2(1 - \delta_p^2/I^P_{zz}) + 2\xi_f \omega_f s + \omega_f^2} \right] \qquad (24)$$

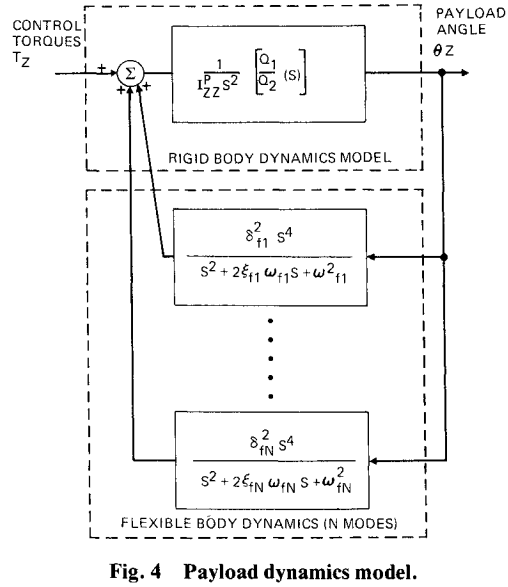

Fig. 4 Payload dynamics model.

For no assumed structural damping (a conservative assumption for analytical interaction studies) the effect of modeling flexibility is to add an additional dipole on the imaginary axis of the s-plane at the mode frequency. The pole-zero separation is a function of the "effective inertia" of the mode δ_f^2 (with $\delta_f^2/I_{zz}^P < 1$). This similarity between the structure of the dynamics describing flexibility and the vehicle nutation mode leads one to investigate the interaction of the control system with the payload flexible dynamics using the technique developed in the previous section to analyze the nutation mode interaction. Again, the root perturbation technique, establishing the closed-loop effect of the composite system dynamics (i.e., all dynamics exclusive of the flexible mode of interest) on the flexible mode will yield the expression for the closed-loop damping time constant of the mode given by,

$$\tau_f = \left[\frac{-2(1-\rho)^{3/2}}{\rho \omega_f} \right] \left[\frac{1+\bar{K}^2+2\bar{K}\cos\alpha}{\bar{K}\sin\alpha} \right] \qquad (25)$$

with $\rho \equiv \delta_f^2/I_{zz}^P$ and $\bar{K} = K/(1-\rho) \simeq K$ for $\rho \ll 1$.

It can be seen there exists a one-to-one correspondence between the interaction effects of the flexible mode effective inertia δ_f^2, and the payload cross-product of inertia, I_{xz}^P. As either δ_f^2 or I_{xz}^P vanish, the system becomes uncoupled from the respective mode, as observed by either the cancellation of the pole and zero in the transfer functions or the infinite time constants from Eqs. (15) and (25). In both cases, the strength of the dynamic interaction (defined by the relative pole-zero separation) is determined by both a well-defined mass property coupling parameter (r or ρ), and the system transmission gain at the mode frequency. In addition, the fundamental stability of the flexible mode/DCS interaction can be determined by observing the system transmission phase angle in a manner identical to the nutation mode analysis described previously. For structural flexibility analysis, the effects of adding a structural damping can be directly related to the effects of a passive damping mechanism on the nutation mode.

For assumed zero structural mode damping, Eq. (25) presents a technique to ensure a "phase" stabilized mode, where the control system can be tuned to ensure maximum active damping. By adjusting the control system dynamics to provide that the open-loop phase angle of the flexible mode frequency lie in the third or fourth quadrants, flexible mode stability is assured. By adjusting the open-loop gain at the mode frequency, the strength of the actig damping can be controlled. The use of notch filters in the control shaping can be introduced to alter the system gain in a particular frequency band, without disturbing other control loop characteristics.

It should be noted here that the flexible mode interaction analysis technique presented here is not restricted to a dual-spin spacecraft application. The dynamic transfer function for an arbitrary body with elastic properties will be represented in the form described by Eq. (24), with the exclusion of the nutation mode. That is, the dynamics can be described by the fundamental rigid body motion plus the elastic modes as shown in Fig. 4. The addition of a feedback control system exhibits the same characteristics as described in the previous sections, and the interaction analysis can be accomplished in the same manner. This will be illustrated with the following examples.

V. Stabilization Techniques—Design Examples

As illustrations of the techniques involved in the design of control systems involving rigid and nonrigid plant dynamics, two examples will be considered. The first describes the design of a typically low bandwidth payload despin control system for the spacecraft illustrated in Fig. 1. The second example deals with a much wider bandwidth control system design for a hypothetical precision pointing experiment which would be mounted on the despun payload. Because of the magnitude of the mass properties of the total vehicle and typical accuracy

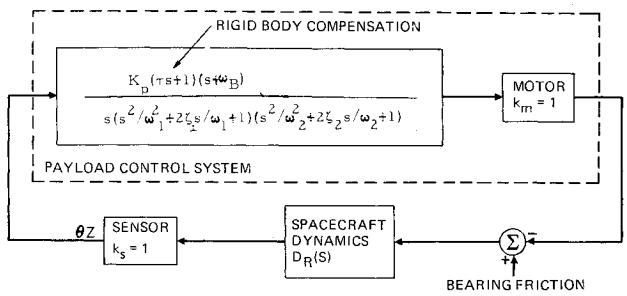

Fig. 5 Payload despin control system analytical model. Control system parameters $K_p = 0.6$ ft/lb/deg, $\tau = 3$ sec, $\omega_B = 0.1$ rad/sec, $\omega_1 = 5$ rad/sec, $\xi_1 = 0.7$, $\omega_2 = 8$ rad/sec, $\xi_2 = 0.4$. Vehicle mass properties: $I_{zz}^P = 100$ slug-ft^2, $I_{zz}^R = 200$ slug ft^2, $I_{xx} = I_{yy} = 1000$ slug-ft^2, $I_{xz}^P = 30$ slug-ft^2, $\omega_{so} = 70$ RPM.

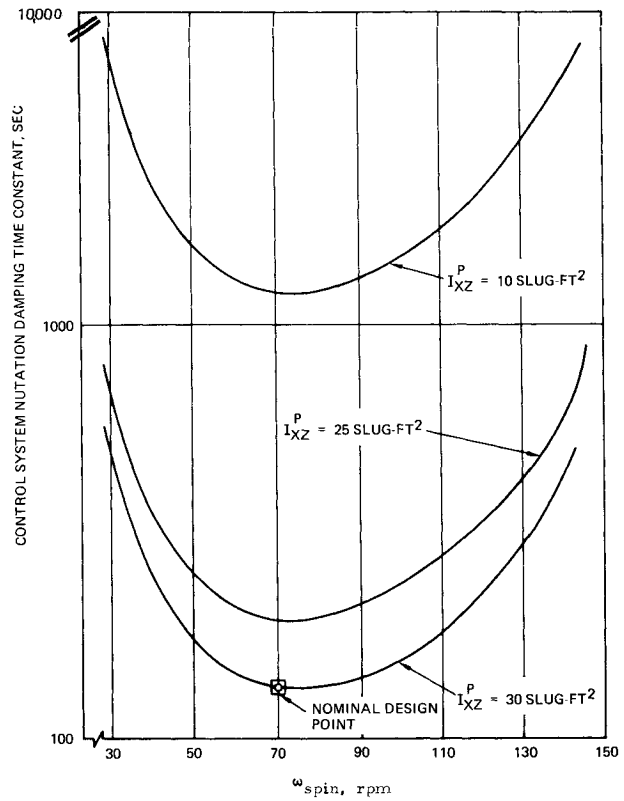

Fig. 6 Closed-loop nutation damping time constant as a function of spin speed and cross product.

requirements, for this example, vehicle nutation frequency will exhibit substantial frequency separation from payload flexible modes. By observing the magnitude characteristics of Eq. (15), it can be shown that the DCS/flexible mode interaction will be very weak. The wider bandwidth payload experiment will, by the same argument, be uncoupled from the low-frequency vehicle nutation, but strongly coupled to the payload flexible dynamics.

The despin control system consists of a static earth sensor mounted on the despun payload. The sensor output is a continuous measurement of the deviation of the despun platform line-of-sight from the center the earth. The output is shaped to derive commands to the torque motor contained in the bearing assembly which provides the spinning/despun interface. The analytical model for the control system is shown in Fig. 5.

Because of the arbitrary mass distribution of the despun payload, a substantial payload cross product of inertia will lead to a potentially strong coupling between the DCS and vehicle nutation. Using frequency domain analysis techniques (i.e., Bode or Nyquist analysis) and the previous results, the DCS shaping parameters were adjusted to provide maximum nutational stability from the control system interaction. The

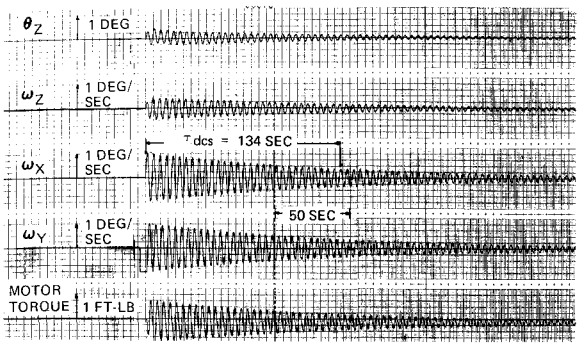

Fig. 7 Nutation transient response.

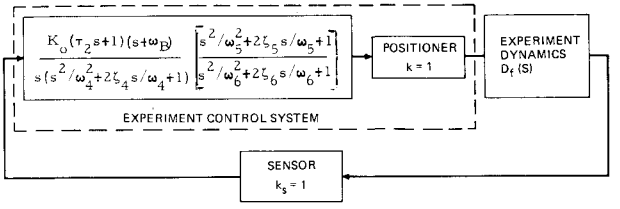

Fig. 8 Precision pointing experiment control system analytical model. Control system parameters: $K_0 = 85$ ft/lb/deg, $\tau_2 = 0.12$ sec, $\omega_B = 1$ rad/sec, $\omega_4 = 80$ rad/sec, $\xi_4 = 1$, $\omega_5 = 80$ rad/sec, $\xi_5 = 0.3$, $\omega_6 = 160$ rad/sec, $\xi_6 = 0.6$. Mass properties: experimental control inertia = 35 slug-ft.^{2} Flexible mode: $f_f = 15.547$ Hz, $\delta_f^2 = 4.55$ slug-ft.^{2}.

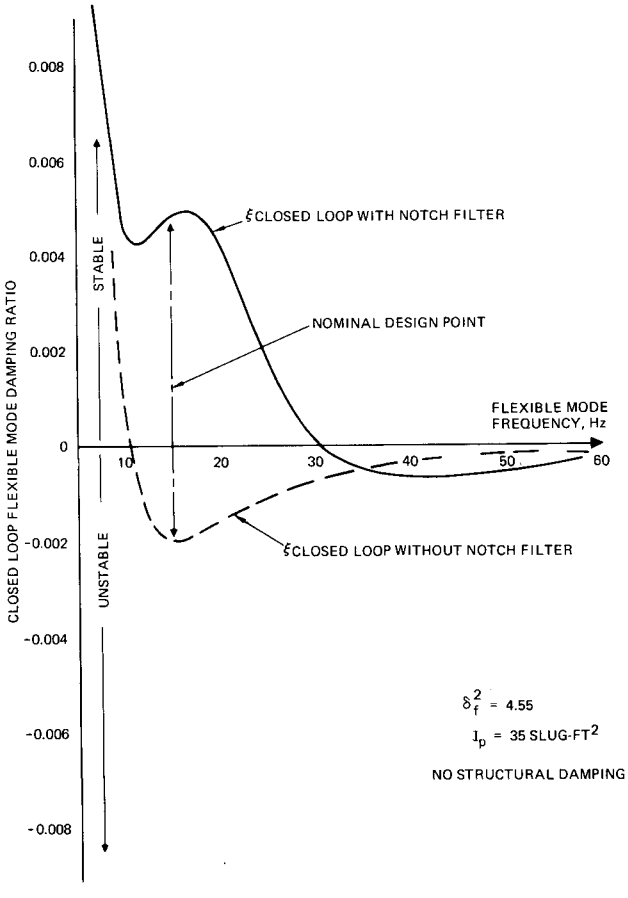

Fig. 9 Closed-loop flexible mode damping as a function of mode frequency.

resulting theoretical closed-loop nutation time constant, τ_{dcs}, as a function of rotor spin rate and for several values of I_{xz}^P is shown in Fig. 6. For the nominal design parameters ($I_{xz}^P = 30$ slug-ft^2 and $\omega_{so} = 70$ rpm), the resulting time constant is 134

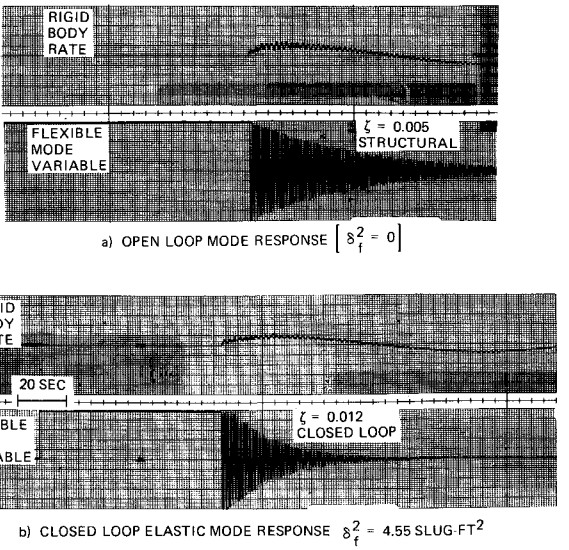

Fig. 10 Flexible mode transient response.

sec which is comparable to the damping available from a strong passive damper.

To verify these results, an analog computer simulation of the DCS was implemented. Figure 7 is a time history showing the closed-loop system response to an initial nutation transient with nominal design parameters.

The control system model for the payload mounted precision pointing experiment is shown in Fig. 8. Here a precision reference is used for continuous tracking of an inertial target (for example, a sun telescope). For the experimen- strongly coupled flexible mode was assumed with a nominal mode frequency of 15.5 Hz, near the bandwidth of the control system. The basic control loop parameters were chosen to meet the experiment performance requirements. However, the elastic mode interaction with the control system is unstable for light structural damping (typically an undetermined parameter). To ensure stability with a conservative assumption of no structural damping, the additional notch filter stage was added to the control system shaping. The effect of the notch dynamics is to alter the system function gain and phase around the mode frequency to ensure the phase angle lines in the third quadrant. The resulting closed-loop modal damping is summarized in Fig. 9. For no assumed structural damping and without the notch filter, the interaction produces a closed damping ratio of $-.2\%$ (unstable). Adding the filter results in a stabilizing interaction with $+.55\%$ damping. The additional filter dynamics provides stable interaction for modes with frequencies to 32 Hz.

An analog computer simulation of this control system was implemented and the results are shown in Fig. 10. Here, the time response of the modal variable to an initial transient is given for both an uncoupled mode ($\delta_f^2 = 0$) and the nominal coupling ($\delta_f^2 = 4.55$ slug-ft^2). For this illustration, a structural damping of 0.5% is assumed. The figure shows the predicted increase in mode damping (to 1.2%) when the control system is coupled to the flexible mode dynamics.

VI. Conclusions

Active control of both nutation and flexibility of a dual-spin spacecraft was discussed. The use of the inherent dynamic coupling through the vehicle mass properties in conjunction with the on-board payload control system can provide substantial active closed loop control. The closed-form expression defining the resulting closed loop active damping time constant can be used to easily evaluate the interaction effects over a wide range of control loop parameters and vehicle mass properties. The expression can also be used to effectively "tune" the control system (within the limits im-

posed by other loop design constraints) to nutation frequency and thus optimize the coupling providing maximum stability margins. The analysis presented also provides a technique to analyze the effects of general flexible body interactions with a feedback control system. Both the stability and strength of the coupling can be evaluated without explicitly including the flexible mode dynamics in the analysis. The closed-form solution for the control-loop modal damping presents a design technique to ensure stability directly without the need for detailed numerical evaluation or simulation. Classical control system graphical techniques (i.e., Bode, Nyquist, or Nichols plots) are sufficient to evaluate the interaction. Extensions of this analysis to more general configurations including sampled-data control systems involving spinning sensors, and including the effects of sensor kinematic coupling paths will be described in a separate paper.

References

[1] Iorillo, A. J., "Analysis Related to the Hughes Gyrostat System," Hughes Aircraft Co. Rept. SSDT0438B, Dec. 1967.

[2] Likins, P. W., "Attitude Stability Criteria for a Dual-Spin Spacecraft," *Journal of Spacecraft and Rockets,* Vol. 4, April 1967, pp. 1638-1643.

[3] Mingori, D.L., "Effects of Energy Dissipation on the Attitude Stability of Dual Spin Satellites," *AIAA Journal,* Vol. 7, Jan. 1969 pp. 20-27.

[4] Neer, J.T., "Intelsat IV Nutation Dynamics," Paper No. 72-537, Washington, D.C., April 1972.

[5] Phillips, K., "Active Nutation Damping Utilizing Spacecraft Mass Properties," *IEEE Transactions on Aerospace and Electronic Systems,* Vol. AES-9 Sept. 1973.

[6] Phillips, K.J., "Linearization of the Closedop Dynamics of a Dual Spin Spacecraft," *Journal of Spacecraft and Rockets,* Vol. 8, Sept. 1971.

[7] Leliakov, I.P. and Barba, P.M., "Damping Spacecraft tation by Means of a Despun Antenna," presented as AAS/AIAA Astrodynamics Conference, Vail Colo., 1973.

[8] Likins, P.W., "Dynamics and Control of Flexible Space Vehicles, Revision 1," Tech. Rept. 32-1329, Jan. 1970, Jet Propulsion Lab., Pasadena, Calif.